

This discussion paper is/has been under review for the journal Biogeosciences (BG).  
Please refer to the corresponding final paper in BG if available.

# Daily burned area and carbon emissions from boreal fires in Alaska

S. Veraverbeke<sup>1</sup>, B. M. Rogers<sup>2</sup>, and J. T. Randerson<sup>1</sup>

<sup>1</sup>University of California, Irvine, California, USA

<sup>2</sup>Woods Hole Research Center, Falmouth, Massachusetts, USA

Received: 7 November 2014 – Accepted: 18 November 2014 – Published: 18 December 2014

Correspondence to: S. Veraverbeke (sander.veraverbeke@uci.edu)

Published by Copernicus Publications on behalf of the European Geosciences Union.

## Daily burned area and carbon emissions from boreal fires in Alaska

S. Veraverbeke et al.

Title Page

Abstract

Introduction

Conclusions

References

Tables

Figures



Back

Close

Full Screen / Esc

Printer-friendly Version

Interactive Discussion



## Abstract

Boreal fires burn carbon-rich organic soils, thereby releasing large quantities of trace gases and aerosols that influence atmospheric composition and climate. To better understand the factors regulating boreal fire emissions, we developed a statistical model of carbon consumption by fire for Alaska with a spatial resolution of 500 m and a temporal resolution of one day. We used the model to estimate variability in carbon emissions between 2001 and 2012. Daily burned area was mapped using imagery from the Moderate Resolution Imaging Spectroradiometer combined with perimeters from the Alaska Large Fire Database. Carbon consumption was calibrated using available field measurements from black spruce forests in Alaska. We built two nonlinear multiplicative models to separately predict above- and belowground carbon consumption by fire in response to environmental variables including elevation, day of burning within the fire season, pre-fire tree cover and the differenced normalized burn ratio (dNBR). Higher belowground consumption occurred later in the season and for mid-elevation regions. Aboveground and belowground consumption also increased as a function of tree cover and the dNBR, suggesting a causal link between the processes regulating these two components of consumption. Between 2001 and 2012, the median fuel consumption was  $2.48 \text{ kg C m}^{-2}$  and the median pixel-based uncertainty (SD of prediction error) was  $0.38 \text{ kg C m}^{-2}$ . There were considerable amounts of burning in other cover types than black spruce and consumption in pure black spruce stands was generally higher. Fuel consumption originated primarily from the belowground fraction (median =  $2.30 \text{ kg C m}^{-2}$  for all cover types and  $2.63 \text{ kg C m}^{-2}$  for pure black spruce stands). Total carbon emissions varied considerably from year to year, with the highest emissions occurring during 2004 (67 TgC), 2005 (44 TgC), 2009 (25 TgC), and 2002 (16 TgC) and a mean of 14 TgC per year between 2001 and 2012. Our analysis highlights the importance of accounting for the spatial heterogeneity within fuels and consumption when extrapolating emissions in space and time. This data on

### Daily burned area and carbon emissions from boreal fires in Alaska

S. Veraverbeke et al.

Title Page

Abstract

Introduction

Conclusions

References

Tables

Figures



Back

Close

Full Screen / Esc

Printer-friendly Version

Interactive Discussion



daily burned area and emissions may be useful for in understanding controls and limits on fire growth, and predicting potential feedbacks of changing fire regimes.

## 1 Introduction

Fire is the most important landscape disturbance in the boreal forest (Chapin et al., 2000; Krawchuk et al., 2006). Increases in the extent and severity of burning in the last several decades have been reported for Alaska and Canada (Gillett et al., 2004; Kasischke and Turetsky, 2006; Kasischke et al., 2010; Turetsky et al., 2011). With accelerated warming predicted for the boreal region during the remainder of the 21st century (Collins et al., 2013), intensification of the fire regime is expected (Amiro et al., 2009; Balshi et al., 2009; de Groot et al., 2013). The interactions between the boreal ecosystem, fire and climate are complex. Boreal fires have both positive and negative climate feedbacks (Randerson et al., 2006; Bowman et al., 2009; Oris et al., 2014). Cooling is primarily caused by the increased surface albedo due to more persistent snow cover and early successional vegetation in burned areas mainly occurring during the spring and winter months (Randerson et al., 2006; Rogers et al., 2013), and organic carbon aerosol effects (Tosca et al., 2013). The emission of greenhouse gases and black carbon aerosols (Bowman et al., 2009), and the deposition of black carbon on snow and ice (Flanner et al., 2007) are the dominant warming feedbacks.

The magnitudes of these feedbacks are tightly linked with the severity of the disturbance (Beck et al., 2011a; Turetsky et al., 2011; Jin et al., 2012). Severity is often referred to in a general way describing the amount of environmental damage that fire causes to an ecosystem (Key and Benson, 2006). In the context of mostly stand-replacing boreal fires, severity is expressed as the degree of consumption of belowground organic matter. Differences in ground layer burn depths control the amount of carbon combusted, and impact post-fire succession trajectories and consequent albedo feedbacks (Johnstone and Kasischke, 2005; Johnstone et al., 2010; Jin et al., 2012). Heterogeneity in fuels, fuel conditions, topography and fire

**BGD**

11, 17579–17629, 2014

### Daily burned area and carbon emissions from boreal fires in Alaska

S. Veraverbeke et al.

Title Page

Abstract

Introduction

Conclusions

References

Tables

Figures



Back

Close

Full Screen / Esc

Printer-friendly Version

Interactive Discussion





## Daily burned area and carbon emissions from boreal fires in Alaska

S. Veraverbeke et al.

Title Page

Abstract

Introduction

Conclusions

References

Tables

Figures



Back

Close

Full Screen / Esc

Printer-friendly Version

Interactive Discussion



the seasonality of the burn (Kajii et al., 2002; Kasischke and Bruhwiler, 2002; Soja et al., 2004). The dryness of the forest floor depends both on the time within the season and local drainage conditions (Kane et al., 2007; Turetsky et al., 2011). Kasischke and Hoy (2012) incorporated this expert knowledge to derive emissions from a set of Alaskan fires by accounting for differential impacts of fire seasonality on several topographic classes.

A complementary approach to derive different levels of fuel consumption is to use direct post-fire remote sensing observations of severity (Kolden and Abatzoglou, 2012; Veraverbeke and Hook, 2013; Rogers et al., 2014). Severity is often referred to as fire or burn severity (Lentile et al., 2006; Keeley, 2009) and the difference between both terms lays within the temporal dimension of the post-fire environment. By definition fire severity measures the immediate impact of the fire, whereas burn severity incorporates both the immediate fire impact and subsequent recovery effects (Lentile et al., 2006; Veraverbeke et al., 2010). Spectral changes after a fire have shown to be strongly related to field measurements of severity in a wide range of ecosystems (e.g. van Wagendonk et al., 2004; Cocke et al., 2005; De Santis and Chuvieco, 2007; Veraverbeke and Hook, 2013), including the boreal forest (Epting et al., 2005; Allen and Sorbel, 2008; Hall et al., 2008; Soverel et al., 2010). In particular the differenced normalized burn ratio (dNBR) has become accepted as the standard spectral index to assess severity (López García and Caselles, 1991; Key and Benson, 2006). The dNBR is an index that combines near and short-wave infrared reflectance values obtained before and after a fire (Eidenshink et al., 2007). The spectral regions in dNBR are especially sensitive to the decrease of vegetation productivity and moisture content after the fire. Because of this, dNBR is a good indicator of aboveground biomass consumption, but may be less effective in estimating belowground consumption of boreal fires (French et al., 2008; Hoy et al., 2008; Kasischke et al., 2008). Other studies, however, have reported significant relationships between spectral indices, including dNBR, and belowground consumption measurements from field sites in boreal ecosystems (Hudak et al., 2007; Verbyla and Lord, 2008; Rogers





fire on the North Slope is the largest tundra fire on record (Jones et al., 2009; Mack et al., 2011; Kolden and Rogan, 2013), and the occurrence of tundra fires may increase with global warming (Hu et al., 2010; Rocha et al., 2012).

## 2.2 Field data

5 We assembled field data from three different publications (Boby et al., 2010; Turetsky et al., 2011; Rogers et al., 2014). Due to limited data availability for other land cover types than black spruce, we focused on black spruce plots and we retained all plots burned since 2000 for which cloud-free one year-post fire dNBR observations were available in the Monitoring Trends in Burn Severity (MTBS, Eidenshink et al., 2007) database, resulting in a total of 126 plots (Table S2 in the Supplement). The location of the field plots is given in Fig. 1. Boby et al. (2010) and Rogers et al. (2014) provided a direct estimate of the belowground carbon consumption representing 39 plots. These plots, except for one of the Boby et al. (2010) plots, also included an estimate of aboveground consumption. Detailed description of the field sites and data acquisition can be found in the respective publications. For the Turetsky et al. (2011) plots, belowground carbon consumption was calculated from depth of burn measurements using separate, region-wide mean soil-carbon accumulation curves for lowland, upland, and slopes with South (S), North (N), and East or West (EW) aspect (Fig. S2). We used a digital elevation model (Sect. 2.3.3) resampled to 500 m resolution for assigning the topographic classes to the field plots. Concave flat (slope  $\leq 2\%$ ) areas were classified as lowland (L), convex flat areas were as upland (U). Sloped terrain was categorized as N aspect (aspect  $\geq 315$  or  $< 45^\circ$ ), S aspect (aspect  $\geq 135$  and  $< 225^\circ$ ), and E or W aspect (aspect  $\geq 45$  and  $< 135^\circ$ , or  $\geq 225$  and  $< 315^\circ$ ).

### Daily burned area and carbon emissions from boreal fires in Alaska

S. Veraverbeke et al.

Title Page

Abstract

Introduction

Conclusions

References

Tables

Figures



Back

Close

Full Screen / Esc

Printer-friendly Version

Interactive Discussion







Vegetation Continuous Fields Collection 5 product at 250 m resolution for the years 2000–2010 (MOD44B, Hansen et al., 2003). The generation of the MOD44B product was discontinued after 2010, and we therefore used the tree cover layer of the year 2010 as pre-fire tree cover for the year 2012.

The time of burning in the season covaries with the mean depth of the active layer, and thus may be related to the amount of dry ground fuels available for burning (Turetsky et al., 2011; Kasischke and Hoy, 2012). We assigned the time of burning for each pixel based on the MODIS active fire observations. We found that the nearest neighbor variant of the inverse distance weighting technique, in which the pixel is assigned the value of the closest active fire detection excluding scan angles larger than 40°, performed best and with a within-one-day accuracy for most pixels (Fig. S3). The resulting progression maps were binned with a daily time step, at local solar time.

We investigated the dNBR as an explanatory variable in our fuel consumption model because extensive literature suggests that it may have some predictive power in boreal forest ecosystems. For the comparison with the field plots, 30 m dNBR data was retrieved from the Landsat-based Monitoring Trends in Burn Severity database (MTBS, Eidenshink et al., 2007). For the statewide extrapolation, we calculated the NBR from MODIS surface reflectance data in the near infrared (NIR, centered at 858 nm) and short-wave infrared (SWIR, centered at 2130 nm) bands:  $NBR = (NIR - SWIR)/(NIR + SWIR)$ . We used the surface reflectance data contained in the 16 day Terra MODIS Vegetation Indices 16 day Collection 5 product at 500 m resolution for the years 2000–2013 (MOD13A1, Huete et al., 2002). To account for cloudy observations in single MODIS composites, we created summer NBR composites using the five 16 day composites between days of the year 177 and 256. We only used good data as indicated by the MOD13A1 quality flags. NBR values were calculated as the mean of all available good observations within the five composites. The dNBR was calculated using the one-year pre-and post-fire NBR layers. Within the MTBS database, we also only considered one-year post-fire dNBR information. This

## BGD

11, 17579–17629, 2014

### Daily burned area and carbon emissions from boreal fires in Alaska

S. Veraverbeke et al.

Title Page

Abstract

Introduction

Conclusions

References

Tables

Figures



Back

Close

Full Screen / Esc

Printer-friendly Version

Interactive Discussion



minimized potential differences in the interpretation of dNBR values from different post-fire years (Veraverbeke et al., 2010).

The above six variables (elevation, slope, northness, tree cover, time of burning and dNBR) were targeted to develop the belowground consumption model. dNBR and tree cover were used as predictors of aboveground consumption.

### 2.3.4 Land cover data

We used the Fuel Characteristic Classification System (FCCS, Ottmar et al., 2007; Riccardi et al., 2007) layer of the year 2001 at 30m to represent land cover in the study area (downloaded from <http://landfire.cr.usgs.gov/viewer/>, last accessed 25 November 2014). The FCCS is a national effort by the U.S. Forest Service to provide a fuel type classification that is compiled from literature, inventories, photo series and expert opinion (Ottmar et al., 2007; Riccardi et al., 2007). For Alaska, the layer is available for the years 2001 and 2008. Since less than one percent of reburning occurred during the period of our study (2001–2012), we decided to only use the 2001 layer. We aggregated the fuel types into five land cover classes: black spruce, white spruce, deciduous, tundra-grass-shrub and non-vegetated (Table S1, Fig. S1).

## 3 Methods

AKFED provides daily burned area and carbon emissions for the state of Alaska between 2001 and 2012 at 500m resolution. Since unburned islands are not fully accounted for within perimeters (Kasischke and Hoy, 2012; Kolden et al., 2012; Rogers et al., 2014; Sedano and Randerson, 2014), and some small fires are not accounted for outside the perimeters (Randerson et al., 2012), we developed a burned area mapping approach that screened dNBR values within the ALFD perimeters and in the vicinity of active fire pixels outside the perimeters.

## Daily burned area and carbon emissions from boreal fires in Alaska

S. Veraverbeke et al.

Title Page

Abstract

Introduction

Conclusions

References

Tables

Figures



Back

Close

Full Screen / Esc

Printer-friendly Version

Interactive Discussion



## Daily burned area and carbon emissions from boreal fires in Alaska

S. Veraverbeke et al.

Title Page

Abstract

Introduction

Conclusions

References

Tables

Figures



Back

Close

Full Screen / Esc

Printer-friendly Version

Interactive Discussion



The carbon consumption model was formulated for black spruce based on the relationship between the observed carbon consumption at the field locations and the environmental variables. We extracted the pixel values of elevation, slope, northness, pre-fire tree cover and dNBR at 30 m at the location of the field plots. The time of burning was assigned from the nearest active fire observation.

To extrapolate the model in space and time, we used a spatial resolution of approximately 500 m, the native resolution of the MOD13A1 product used to derive the dNBR layers. The exact spatial resolution of AKFED is 450 m, which is the multiple of 30 m closest to the exact 463 m native resolution of the MOD13A1 product. This spatial resolution facilitated spatial averaging of 30 m DEM, tree cover and land cover data, and is referred to in this manuscript as 500 m. The decision to extrapolate the model at this resolution was driven by data availability. We aimed at complete spatial coverage. Even with current efforts such as MTBS and the Web-Enabled Landsat Data (WELD, Roy et al., 2010), initial exploration of these datasets indicated that complete Landsat dNBR coverage for every burned pixel was still partly constrained by clouds, smoke, snow and gaps due to the Landsat 7 scan line corrector failure.

Elevation, aspect and northness were spatially averaged from the native 30 m resolution of the ASTER GDEM 2 to the 500 m resolution. Similarly, the MOD44B tree cover product was spatially averaged from its native 250 m resolution to the 500 m resolution. The time of burning was also obtained at this grid resolution. To account for other land cover types than black spruce, the aggregated FCCS product was rescaled to 500 m in a way that every pixel at 500 m contained the percentage of black spruce, white spruce, deciduous, tundra-grass-shrub and non-vegetated land (Fig. S1). All analyses were performed within the Albers equal area projection for Alaska (central meridian: 154° W, standard parallel 1: 55° N, standard parallel 2: 65° N, latitude of origin: 50° N) with North American Datum 1983 (NAD83). An overview of the workflow is given in Fig. 2.

We compared the yearly burned area and carbon emissions estimates derived from AKFED with those from GFED3s (Randerson et al., 2012), and therefore spatially

averaged the AKFED estimates over the 0.25° grid from GFED3s for the period 2001–2010.

### 3.1 Daily burned area mapping (500 m)

Annual burned area maps at 500 m were derived by applying a threshold on the dNBR values of pixels within the perimeters of the ALFD and outside the perimeters but within 1 km of an active fire pixel. If a fraction of the 500 m pixel was covered by a fire perimeter polygon, then this pixel was considered in the perimeter. Pixels with a dNBR value larger than 0.15 were classified as burned. The dNBR threshold was determined based on the dNBR variability that exists within unburned pseudo-invariant pixels (100% barren pixels at 500 m, FCCS code 931). We found that, as expected, that the mean dNBR was close to zero (0.01). The SD of the distribution equaled 0.15. By selecting this value as our threshold for the burned area mapping, we aimed to minimize commission errors, however, we recognize that this may have incurred a small omission error for pixels that were only partially burned and/or burned with low severity. The threshold value we used was the same as the one applied by Sedano and Randerson (2014) who used a similar burned area mapping approach within ALFD perimeters. All burned pixels were assigned a time of burning from the detection time of the nearest active fire observation excluding observations with view zenith angles higher than 40° (Fig. S3).

### 3.2 Carbon consumption model (30 m)

We aimed to separately predict below- and aboveground carbon consumption based on the relationships between field plot data and environmental variables at 30 m (elevation, slope, northness, pre-fire tree cover, time of burning and dNBR). We investigated two modeling techniques to formulate a carbon prediction model. The first technique was multiplicative nonlinear regression. This technique is based directly on the interpretation of empirical relationships that may exist between the environmental

## Daily burned area and carbon emissions from boreal fires in Alaska

S. Veraverbeke et al.

Title Page

Abstract

Introduction

Conclusions

References

Tables

Figures



Back

Close

Full Screen / Esc

Printer-friendly Version

Interactive Discussion



## Daily burned area and carbon emissions from boreal fires in Alaska

S. Veraverbeke et al.

Title Page

Abstract

Introduction

Conclusions

References

Tables

Figures

◀

▶

◀

▶

Back

Close

Full Screen / Esc

Printer-friendly Version

Interactive Discussion



variables and the carbon consumption field data. This technique has demonstrated to be effective in a similar application to predict fire occurrence and size in Southern California (Jin et al., 2014). The second technique was gradient boosting of regression trees. We applied this technique because previous work indicated that it may have value in predicting depth of burning in boreal black spruce forest (Barrett et al., 2010, 2011). Gradient boosting is a machine learning technique, which produces a prediction model in the form of an ensemble of, in our case, multiple regression trees. We parameterized the gradient boosting of regression trees with the requirement that each leaf of at least 10% of the data per leaf and using 50 weak learner trees. Both multiplicative nonlinear regression and gradient boosting of regression trees allow for nonlinear relationships between the dependent and independent variables, and interactions between the independent variables. We opted to use the multiplicative nonlinear regression model for our study because we found it to outperform the gradient boosting model in predicting observations that were not used to train the models (Fig. S4).

### 3.3 Daily carbon emissions, 2001–2012 (500 m)

Once the carbon consumption prediction model was optimized, we extrapolated this model over the spatiotemporal domain of the study at 500 m resolution. To do so, we first quantified the linear relationship between Landsat and MODIS dNBR and tree cover (Fig. S5). The resulting regression equations were applied to the MODIS-derived dNBR and tree cover layers to allow direct application in the carbon consumption model that was optimized using Landsat data.

Due to data paucity of carbon consumption in other land cover types than black spruce, we were only able to formulate a prediction model for black spruce forest. Deciduous and white spruce stands generally have higher aboveground and lower belowground fuel loads (Kasischke and Hoy, 2012; Rogers et al., 2014). We assumed that fuel consumption in these land cover types was controlled by the same variables as from the black spruce consumption model. However, we multiplied the estimates



cover ( $R_{\text{adjusted}}^2 = 0.03$ ,  $p < 0.05$ ) had a weaker influence (Fig. S8). The aboveground carbon consumption demonstrated stronger, also exponential, relationships with pre-fire tree cover ( $R_{\text{adjusted}}^2 = 0.53$ ,  $p < 0.001$ ) and dNBR ( $R_{\text{adjusted}}^2 = 0.23$ ,  $p < 0.001$ ) variables (Fig. S9).

The optimized multiplicative nonlinear model for the depth of burn and belowground carbon consumption in black spruce forest based on the field and 30 m data was formulated as:

$$\text{depth}_{30\text{ m}} \text{ or } C_{\text{belowground},30\text{ m}} = c_1 + c_2 \cdot e^{c_3 \cdot \text{dNBR}} \cdot e^{c_4 \cdot \text{tc}} e^{c_5 \cdot \text{DOY}} \cdot e^{-\frac{(\text{elev}-c_6)^2}{2 \cdot c_7}} \quad (2)$$

where  $c_{1,\dots,7}$  are the optimized coefficients, dNBR is the differenced normalized burn ratio, tc is the pre-fire tree cover, DOY is the day of the year and elev is the elevation. This model yielded a  $R_{\text{adjusted}}^2$  of 0.40 and a root mean square error (RMSE) of 5.44 cm ( $p < 0.001$ ) for depth of burn (Fig. 3a) and a  $R_{\text{adjusted}}^2$  of 0.29 and a RMSE of  $1.99 \text{ kg C m}^{-2}$  ( $p < 0.001$ ) for belowground carbon consumption (Fig. 3c). Inclusion of slope and northness did not improve the performance of the models.

The aboveground carbon consumption in black spruce forest was modeled as a multiplicative exponential model of the 30 m dNBR and pre-fire tree cover variables:

$$C_{\text{aboveground},30\text{ m}} = c_1 + c_2 \cdot e^{c_3 \cdot \text{dNBR}} \cdot e^{c_4 \cdot \text{tc}} \quad (3)$$

where  $c_{1,\dots,4}$  are the optimized coefficients. This model had a  $R_{\text{adjusted}}^2$  of 0.53 and a RMSE of  $0.26 \text{ kg C m}^{-2}$  ( $p < 0.001$ ) (Fig. 3e), the same as the individual relationship between the aboveground carbon consumption and pre-fire tree cover. In the mostly stand-replacing fires that occur in black spruce forest, dNBR did not contribute to the aboveground model. However, we decided to include dNBR to allow for variations in the severity of burning in other land cover types than black spruce, for example in deciduous stands which often burn less severe and frequent (Viereck, 1973; Cumming, 2001). We found no trends in the residuals of any of the models (Fig. 3b, d and f). The

Daily burned area and carbon emissions from boreal fires in Alaska

S. Veraverbeke et al.

Title Page

Abstract

Introduction

Conclusions

References

Tables

Figures

⏪

⏩

◀

▶

Back

Close

Full Screen / Esc

Printer-friendly Version

Interactive Discussion



environmental variables used in the carbon consumption models are plotted for the spatiotemporal domain in Fig. S10.

Using the consumption ratios derived for white spruce and deciduous cover (Fig. S6), below- and aboveground carbon consumption at 500 m resolution were calculated as:

$$C_{\text{belowground},500\text{ m}} = (fr_{\text{bs}} + 0.66 \cdot fr_{\text{ws}} + 0.31 \cdot fr_{\text{dec}}) \cdot C_{\text{belowground},30\text{ m}} \quad (4)$$

$$C_{\text{aboveground},500\text{ m}} = (fr_{\text{bs}} + 1.56 \cdot fr_{\text{ws}} + 1.75 \cdot fr_{\text{dec}}) \cdot C_{\text{aboveground},30\text{ m}} \quad (5)$$

where  $fr_{\text{bs}}$  is the fraction of black spruce within the 500 m pixel,  $fr_{\text{ws}}$  is the fraction of white spruce and  $fr_{\text{dec}}$  is the fraction of deciduous. The black spruce model was also applied to residual tundra-grass-shrub and non-vegetated parts of each pixel. Before application in Eqs. (4) and (5), the dNBR and tree cover from MODIS were first converted into their Landsat equivalent values using the equations from Fig. S5. The total carbon consumption was calculated as the sum of the below- and aboveground consumption.

To assess the importance of the individual variables in the model we compared all models inputting two or more variables for the depth of burn and belowground consumption models (Fig. 4). For the depth of burn model, elevation was the most important explanatory variable. 2-variables models combining elevation with time of burning and dNBR for example performed better than the 3-variables models that excluded elevation. For the belowground consumption model, the time of burning variable was crucial. All 2-variables models combining time of burning with any of the other variables performed better than the 3-variables models that excluded time of burning.

## 4.2 Daily burned area and carbon emissions, 2001–2012

The total carbon emissions and uncertainty for the spatiotemporal domain are shown in Figs. 5 and 6. Daily carbon emissions over the entire spatial domain were primarily driven by daily burned area (Fig. 6), however, there was considerably spatial variability

### Daily burned area and carbon emissions from boreal fires in Alaska

S. Veraverbeke et al.

Title Page

Abstract

Introduction

Conclusions

References

Tables

Figures

⏪

⏩

◀

▶

Back

Close

Full Screen / Esc

Printer-friendly Version

Interactive Discussion





field data also had a higher median elevation, tree cover and dNBR compared to the distribution of the burned area between 2001 and 2012 (Fig. S11).

Yearly burned area and carbon emissions from AKFED and GFED3s were similar in all years except 2001 (Table S3) when MODIS experienced an outage (Giglio et al., 2013). A strong linear relationship existed between the annual spatial distribution of AKFED and GFED3s 0.25° burned area between 2001 and 2010 ( $r = 0.95$ , intercept = 0.04 and slope = 0.98). The similarity between the burned area from AKFED and GFED3s is not surprising since they operate with similar algorithms. Both algorithms look at changes in a spectral index derived from MODIS surface reflectance imagery within a spatial context that is known to have high burned area probability. GFED3s therefore exclusively relies on the MODIS active fire data, while AKFED made combined use of the perimeters of the ALFD and MODIS active fire data outside the perimeters. Carbon emissions were also closely related between the two products ( $r = 0.87$ , intercept = 0 and slope = 0.79), as well as mean consumption (2.48 kg C m<sup>-2</sup> for AKFED vs. 2.57 kg C m<sup>-2</sup> for GFED3s). Statistics of individual years generally followed these trends, except for the year 2001. AKFED and GFED3s exhibited no significant spatial correlation for carbon consumption ( $r = -0.04$ ,  $p = 0.13$ ). The difference between the consumption estimates from GFED3s and AKFED is likely a consequence of the different parametrization of belowground consumption in the two products. GFED3s estimates organic layer consumption in boreal soils directly as a function of soil moisture (van der Werf et al., 2010). AKFED uses elevation and time of burning to estimate soil moisture, and is complemented with pre-fire tree cover and post-fire dNBR data. The difference in spatial resolution between AKFED (500 m) and GFED3s (0.25°) may also explain part of the discrepancy.

## BGD

11, 17579–17629, 2014

### Daily burned area and carbon emissions from boreal fires in Alaska

S. Veraverbeke et al.

Title Page

Abstract

Introduction

Conclusions

References

Tables

Figures

◀

▶

◀

▶

Back

Close

Full Screen / Esc

Printer-friendly Version

Interactive Discussion



## 5 Discussion

### 5.1 Burned area

Our results corroborate previous work highlighting the importance of unburned islands, which amounted to 18 % of the fire perimeters. This value is close to the estimates of 14, 15 and 17 % reported by Kolden et al. (2012), Sedano and Randerson (2014) and Rogers et al. (2014) for fires in interior Alaska. Burned area and emissions peaked in July and August and extended later in the fire season than previously reported for burning before the 2000s (Kasischke et al., 2002) (Fig. 7b). This tendency towards late-season burning was found for the four largest fire years that occurred during the study period (2002, 2004, 2005 and 2009) (Fig. 6) and can be attributed to the late-season occurrence of weather conditions favorable to fire spread during these large fire years (Hu et al., 2010; Sedano and Randerson, 2014). Some of these late-season fires have occurred outside the fire-sensitive region of interior Alaska which is dominated by black spruce forest. The large Anaktuvuk River fire of 2007 on the North Slope is a well-known example of this (Hu et al., 2010; Mack et al., 2011; Rocha et al., 2012). This suggests that late-season fires may increasingly occur in sparsely vegetated areas like tundra that, despite low aboveground biomass, contain large belowground carbon stocks.

### 5.2 Environmental variables controlling carbon consumption

#### 5.2.1 Elevation

Elevation was the most important variable in the depth of burn model and contributed to the skill of the belowground carbon consumption model (Fig. 4). Barrett et al. (2010, 2011) and Turetsky et al. (2011) demonstrated the explanatory power of topographic variables for belowground consumption in black spruce forests. Kasischke and Hoy (2012) elaborated on their findings and assigned curves of carbon consumption that

BGD

11, 17579–17629, 2014

## Daily burned area and carbon emissions from boreal fires in Alaska

S. Veraverbeke et al.

Title Page

Abstract

Introduction

Conclusions

References

Tables

Figures

⏪

⏩

◀

▶

Back

Close

Full Screen / Esc

Printer-friendly Version

Interactive Discussion



## Daily burned area and carbon emissions from boreal fires in Alaska

S. Veraverbeke et al.

Title Page

Abstract

Introduction

Conclusions

References

Tables

Figures



Back

Close

Full Screen / Esc

Printer-friendly Version

Interactive Discussion



linearly increased with time of burning throughout the fire season to three different topographic classes. The predictive power of elevation for belowground consumption is likely explained by two effects. Elevation captures the spatial distribution of cold temperatures that limit the development of soils and black spruce establishment at the higher elevations (Fig. S7a). Elevation also captures the fuel moisture controls resulting in generally wetter fuels at lower elevations. This moisture control is dynamic through the fire season and this is captured by interactions between elevation and time of burning (Fig. 4). Inclusion of the northness and slope variables did not improve our model prediction. This contrasts with the findings of Barrett et al. (2010, 2011) who ranked slope and aspect, and derived drainage indicators, in the top predictors for depth of burn. It contrasts with Turetsky et al. (2011) who found differences in average consumption among different aspect classes. As an individual variable, slope did display some explanatory power (Figs. S7b and S8b), but did not contribute to the final model. The contrasting findings of this study compared to Barrett et al. (2010, 2011) and Turetsky et al. (2011) can partly be explained by the scale-dependency of controls on carbon consumption. The model in this study was developed for regional state-wide emission predictions. At this scale, the topographic variable explaining most of the variability in belowground fuel consumption (as a proxy of drainage condition and soil organic layer thickness) was elevation. At a more local scale, for example within one fire, differences in elevation may be smaller, and the variability in drainage conditions and hence belowground fuel consumption may be better captured by including slope and aspect variables. Hollingsworth et al. (2006) found a similar scale-dependency explaining the occurrence and abundance of black spruce types from local to regional scales. Further improvements of the model could include fine scale drainage effects driven by slope and aspect superimposed on the elevation control on consumption.

### 5.2.2 Time of burning

Time of burning within the fire season was the most important variable in the belowground carbon consumption model (Fig. 4). Time of burning is used as a proxy



### 5.2.3 Burn severity (dNBR)

The utility of dNBR in the boreal region has been subject to much debate (French et al., 2008). We found a relatively strong relationship between dNBR and aboveground consumption (Fig. S9a). The criticism on the use of dNBR, however, has focused on its ability to predict belowground consumption (French et al., 2008; Hoy et al., 2008). Some authors have found relatively strong correlations between field measures of belowground consumption and dNBR (Hudak et al., 2007; Verbyla and Lord, 2008; Rogers et al., 2014). Barrett et al. (2011) also ranked dNBR in the top third predictors of a set of 35 spectral and non-spectral environmental variables. French et al. (2008) concluded that the use satellite-based assessments of burn severity, including dNBR, in the boreal region “need to be used judiciously and assessed for appropriateness based on the users’ needs”. We found here that, as an individual variable, dNBR was the top predictor of depth of burn in black spruce forests together with pre-fire tree cover (Fig. S7). We also found that including dNBR in the model resulted in additional explained variance compared to models that excluded dNBR (Fig. 4). In addition, dNBR and tree cover were found to vary at a finer spatial scale than elevation or time of burning (Fig. S12), and their inclusion in the model as such likely improved the representation of the spatial heterogeneity in fuel consumption.

The relatively high correlations between depth of burn, and dNBR and tree cover suggest that crown fires in high density black spruce plots also cause deeper burning into the ground layer. Burning into the ground layer is primarily controlled by fuel moisture in the ground layer, which was modeled here as a function of elevation and time of burning. For a certain moisture condition of the ground layer, determined by elevation and fire seasonality, dNBR thus adds complementary power for the prediction of the consumption of the ground layer. This may explain why the dNBR has performed well in studies that focused on one single fire in which the elevation and time of burning were relatively constant (Hudak et al., 2007; Verbyla and Lord, 2008; Rogers et al., 2014). We conclude that the dNBR can well be used as a stand-alone indicator of

## Daily burned area and carbon emissions from boreal fires in Alaska

S. Veraverbeke et al.

Title Page

Abstract

Introduction

Conclusions

References

Tables

Figures



Back

Close

Full Screen / Esc

Printer-friendly Version

Interactive Discussion





---

**Daily burned area and carbon emissions from boreal fires in Alaska**S. Veraverbeke et al.

---

[Title Page](#)[Abstract](#)[Introduction](#)[Conclusions](#)[References](#)[Tables](#)[Figures](#)[◀](#)[▶](#)[◀](#)[▶](#)[Back](#)[Close](#)[Full Screen / Esc](#)[Printer-friendly Version](#)[Interactive Discussion](#)

fraction burned of 61 % (39 % black spruce and 22 % white spruce), a tundra-grass-shrub fraction of 23 %, and a deciduous fraction of 14 %. Although deciduous and white spruce trees may have higher amounts of available aboveground fuel (Kasischke and Hoy, 2012; Rogers et al., 2014), it is well known that the belowground consumption of fuels dominates in boreal ecosystems and that the largest fire-affected belowground carbon stocks are stored in black spruce ecosystems (McGuire et al., 2009; Kasischke and Hoy, 2012). The burning in other land cover types than black spruce thus partly explains the relatively low state-wide median belowground consumption estimate of  $2.3 \text{ kgCm}^{-2}$ . We here used the FCCS classification to characterize land cover. We found this layer indicative for the vegetation patterns in the region. However, we found that 60 out of the 126 black spruce plots from the field dataset (Sect. 2.2) were misclassified as white spruce (29), tundra-grass-shrub (14), deciduous (12) and non-vegetated (5). We also found that of eight white spruce-aspen plots from Rogers et al. (2014), seven were classified as black spruce and one as shrub-grass-tundra. The sample size of the land cover ground truth data available was too small to robustly quantify potential over- or underrepresentation of land cover types in the FCCS layer. An improved land cover characterization, including quantitative uncertainty estimates, is thus essential for reducing region-wide uncertainties. An underrepresentation of the black spruce cover in the FCCS would result in lower state-wide average consumption estimates and vice versa. While some land cover types, such as spruce and deciduous cover, are likely well separable from remote sensing based on spectral and phenological characteristics, more detailed distinctions, for example between black and white spruce, may be more challenging but not impossible with the combined use of structural and optical attributes (e.g. Goetz et al., 2010).

The median belowground consumption estimate increased to  $2.63 \text{ kgCm}^{-2}$  in pure black spruce stands (Fig. 10). This value was still clearly lower than the median of  $3.1 \text{ kgCm}^{-2}$  from the field data used in this study. The field data were, relative to the state wide distribution, disproportionately sampled in mid-elevation areas with high tree cover and high dNBR (Fig. 11s). This suggests that currently available field



discontinuities and fire weather conditions (Krawchuk et al., 2006). Knowledge of these constraints on fire spread may prove valuable when predicting future fire regimes that will result from changes in fire weather, vegetation dynamics and inherent landscape heterogeneity.

At least two aspects of the boreal fire regime in Alaska have already changed over the last half century (Kasischke et al., 2010). There has been an increase in the burned area, driven by a few excessively large fire years, and a shift towards more severe late-season burning. Both changes, however, also provoke additional increases in the surface albedo through deciduous dominance in the early stages of succession and this effect lasts for many decades (Randerson et al., 2006; Johnstone et al., 2010; Barrett et al., 2011; Beck et al., 2011a). Jin et al. (2012) showed that the observed albedo increase scaled with the severity of burning, while Randerson et al. (2006) demonstrated that boreal forest fires can have a slight cooling effect on the climate. The net effect of boreal fires on radiative forcing will have to come from an analysis that integrates the warming, mainly from greenhouse gas emissions, and cooling, mainly from albedo increases, effects over multiple decades with consideration for the spatial heterogeneity in fuels and their consumption.

Fire emission databases with high temporal and spatial resolution also may enable improvements in our understanding of fire aerosol composition and decrease the large uncertainties that currently exist in fire emission factors of different gas species by comparing them to in situ measurements. Fire emission estimates and atmospheric transport models therefore need to be convolved at high spatial and temporal resolution. In addition, fires in the boreal region are episodic and most of the burned area and emissions occur in relatively short amount of time. High resolution time series are therefore of paramount importance as input to transport models and to infer and forecast possible health effects in populated areas exposed to smoke plumes (Hyer et al., 2007).

---

**Daily burned area  
and carbon  
emissions from  
boreal fires in Alaska**

S. Veraverbeke et al.

---

Title Page

Abstract

Introduction

Conclusions

References

Tables

Figures



Back

Close

Full Screen / Esc

Printer-friendly Version

Interactive Discussion





and dNBR and tree cover, suggest a mechanism where high density black spruce plots provide an easier heat transfer of fire from the canopy to the ground layer, and vice versa, resulting in higher consumptions.

The Alaskan Fire Emissions Database (AKFED) is available from [sites.google.com/a/uci.edu/sander-veraverbeke/akfed](http://sites.google.com/a/uci.edu/sander-veraverbeke/akfed) and will be updated regularly. This data could further contribute to the knowledge on spatiotemporal patterns, controls and limits on fire progression, air pollution and exposure, and aerosol composition of boreal fires.

**The Supplement related to this article is available online at  
doi:10.5194/bgd-11-17579-2014-supplement.**

*Author contributions.* S. Veraverbeke designed the study, performed the analyses and wrote the manuscript with inputs from B. M. Rogers and J. T. Randerson at all stages.

*Acknowledgements.* This work was funded by the National Aeronautics and Space Administration Carbon in Arctic Reservoirs Vulnerability Experiment (CARVE) and NNX11AF96G project. We would like to thank the authors from the Boby et al. (2010) and Turetsky et al. (2011) papers for making their field data publicly available. We are also grateful to several colleagues of the University of California, Irvine for discussions on the work.

## References

- Abatzoglou, J. T. and Kolden, C. A.: Relative importance of weather and climate on wildfire growth in interior Alaska, *Int. J. Wildland Fire*, 20, 479–486, doi:10.1071/WF10046, 2011.
- Allen, J. L. and Sorbel, B.: Assessing the differenced Normalized Burn Ratio's ability to map burn severity in the boreal forest and tundra ecosystems of Alaska's national parks, *Int. J. Wildland Fire*, 17, 463–475, doi:10.1071/WF08034, 2008.
- Amiro, B. D., Todd, J. B., Wotton, B. M., Logan, K. A., Flannigan, M. D., Stocks, B. J., Mason, J. A., Martell, D. L., and Hirsch, K. G.: Direct carbon emissions from Canadian forest fires, 1959–1999, *Can. J. For. Res.*, 31, 512–525, doi:10.1139/cjfr-31-3-512, 2001.

## Daily burned area and carbon emissions from boreal fires in Alaska

S. Veraverbeke et al.

[Title Page](#)

[Abstract](#)

[Introduction](#)

[Conclusions](#)

[References](#)

[Tables](#)

[Figures](#)

[⏪](#)

[⏩](#)

[◀](#)

[▶](#)

[Back](#)

[Close](#)

[Full Screen / Esc](#)

[Printer-friendly Version](#)

[Interactive Discussion](#)



- Amiro, B. D., Cantin, A., Flannigan, M. D., and de Groot, W. J.: Future emissions from Canadian boreal forest fires, *Can. J. For. Res.*, 39, 383–395, doi:10.1139/X08-154, 2009.
- Balshi, M. S., McGuire, A. D., Duffy, P., Flannigan, M., Walsh, J., and Melillo, J.: Assessing the response of area burned to changing climate in western boreal North America using a Multivariate Adaptive Regression Splines (MARS) approach, *Glob. Chang. Biol.*, 15, 578–600, doi:10.1111/j.1365-2486.2008.01679.x, 2009.
- Barrett, K., Kasischke, E. S., McGuire, A. D., Turetsky, M. R., and Kane, E. S.: Modeling fire severity in black spruce stands in the Alaskan boreal forest using spectral and non-spectral geospatial data, *Remote Sens. Environ.*, 114, 1494–1503, doi:10.1016/j.rse.2010.02.001, 2010.
- Barrett, K., McGuire, A. D., Hoy, E. E., and Kasischke, E. S.: Potential shifts in dominant forest cover in interior Alaska driven by variations in fire severity, *Ecol. Appl.*, 21, 2380–2396, 2011.
- Beck, P. S. A., Goetz, S. J., Mack, M. C., Alexander, H. D., Jin, Y., Randerson, J. T., and Loranty, M. M.: The impacts and implications of an intensifying fire regime on Alaskan boreal forest composition and albedo, *Glob. Change Biol.*, 17, 2853–2866, doi:10.1111/j.1365-2486.2011.02412.x, 2011a.
- Beck, P. S. A., Juday, G. P., Alix, C., Barber, V. A., Winslow, S. E., Sousa, E. E., Heiser, P., Herriges, J. D., and Goetz, S. J.: Changes in forest productivity across Alaska consistent with biome shift, *Ecol. Lett.*, 14, 373–9, doi:10.1111/j.1461-0248.2011.01598.x, 2011b.
- Beer, T.: The interaction of wind and fire, *Bound.-Lay. Meteorol.*, 54, 287–308, 1991.
- Boby, L. A., Schuur, E. A. G., Mack, M. C., Verbyla, D., and Johnstone, J. F.: Quantifying fire severity, carbon, and nitrogen emissions in Alaska's boreal forest, *Ecol. Appl.*, 20, 1633–1647, doi:10.1890/08-2295.1, 2010.
- Bonan, G. B.: Environmental factors and ecological processes controlling vegetation patterns in boreal forests, *Landscape Ecol.*, 3, 111–130, doi:10.1007/BF00131174, 1989.
- Bowman, D. M. J. S., Balch, J. K., Artaxo, P., Bond, W. J., Carlson, J. M., Cochrane, M. A., D'Antonio, C. M., Defries, R. S., Doyle, J. C., Harrison, S. P., Johnston, F. H., Keeley, J. E., Krawchuk, M. A., Kull, C. A., Marston, J. B., Moritz, M. A., Prentice, I. C., Roos, C. I., Scott, A. C., Swetnam, T. W., van der Werf, G. R., and Pyne, S. J.: Fire in the Earth system, *Science*, 324, 481–484, doi:10.1126/science.1163886, 2009.
- Chapin, F. S., McGuire, A. D., Randerson, J., Pielke, R., Baldocchi, D., Hobbie, S. E., Roulet, N., Eugster, W., Kasischke, E., Rastetter, E. B., Zimov, S. A., and Running, S. W.: Arctic and

## Daily burned area and carbon emissions from boreal fires in Alaska

S. Veraverbeke et al.

Title Page

Abstract

Introduction

Conclusions

References

Tables

Figures



Back

Close

Full Screen / Esc

Printer-friendly Version

Interactive Discussion



boreal ecosystems of western North America as components of the climate system, *Glob. Change Biol.*, 6, 211–223, doi:10.1046/j.1365-2486.2000.06022.x, 2000.

Cocke, A. E., Fulé, P. Z., and Crouse, J. E.: Comparison of burn severity assessments using Differenced Normalized Burn Ratio and ground data, *Int. J. Wildland Fire*, 14, 189–198, doi:10.1071/WF04010, 2005.

Collins, M., Knutti, R., Arblaster, J., Dufresne, J.-L., Fichefet, T., Friedlingstein, P., Gao, X., Gutowski, W. J., Johns, T., Krinner, G., Shongwe, M., Tebaldi, C., Weaver, A. J., and Wehner, M.: Long-term climate change: projections, commitments and irreversibility, in: *Climate Change 2013: The Physical Science Basis. Contributions of Working group I to the Fifth Assessment Report of the Intergovernmental Panel on Climate Change*, edited by: Stocker, F. T., Qin, D., Plattner, G.-K., Tignor, M., Allen, S. K., Boschung, J., Nauels, A., Xia, Y., Bex, V., and Midgley, P. M., Cambridge University Press, Cambridge, United Kingdom, 1029–1136, 2013.

Cumming, S.: Forest type and wildfire in the Alberta boreal mixedwood: what do fires burn?, *Ecol. Appl.*, 11, 97–110, 2001.

De Groot, W. J., Landry, R., Kurz, W. A., Anderson, K. R., Englefield, P., Fraser, R. H., Hall, R. J., Banfield, E., Raymond, D. A., Decker, V., Lynham, T. J., and Pritchard, J. M.: Estimating direct carbon emissions from Canadian wildland fires, *Int. J. Wildland Fire*, 16, 593–606, doi:10.1071/WF06150, 2007.

De Groot, W. J., Pritchard, J. M., and Lynham, T. J.: Forest floor fuel consumption and carbon emissions in Canadian boreal forest fires, *Can. J. For. Res.*, 39, 367–382, doi:10.1139/X08-192, 2009.

De Groot, W. J., Flannigan, M. D., and Cantin, A. S.: Climate change impacts on future boreal fire regimes, *For. Ecol. Manage.*, 294, 35–44, doi:10.1016/j.foreco.2012.09.027, 2013.

De Santis, A. and Chuvieco, E.: Burn severity estimation from remotely sensed data: performance of simulation vs. empirical models, *Remote Sens. Environ.*, 108, 422–435, doi:10.1016/j.rse.2006.11.022, 2007.

Duffy, P. A., Epting, J., Graham, J. M., Rupp, T. S., and McGuire, A. D.: Analysis of Alaskan burn severity patterns using remotely sensed data, *Int. J. Wildland Fire*, 16, 277–284, doi:10.1071/WF06034, 2007.

Eidenshink, J., Schwind, B., Brewer, K., Zhu, Z., Quayle, B., and Howard, S.: A project for monitoring trends in burn severity, *Fire Ecol.*, 3, 3–21, 2007.

## Daily burned area and carbon emissions from boreal fires in Alaska

S. Veraverbeke et al.

Title Page

Abstract

Introduction

Conclusions

References

Tables

Figures

◀

▶

◀

▶

Back

Close

Full Screen / Esc

Printer-friendly Version

Interactive Discussion

Epting, J., Verbyla, D., and Sorbel, B.: Evaluation of remotely sensed indices for assessing burn severity in interior Alaska using Landsat TM and ETM+, *Remote Sens. Environ.*, 96, 328–339, doi:10.1016/j.rse.2005.03.002, 2005.

Flanner, M. G., Zender, C. S., Randerson, J. T., and Rasch, P. J.: Present-day climate forcing and response from black carbon in snow, *J. Geophys. Res.*, 112, D11202, doi:10.1029/2006JD008003, 2007.

French, N. H. F.: Uncertainty in estimating carbon emissions from boreal forest fires, *J. Geophys. Res.*, 109, D14S08, doi:10.1029/2003JD003635, 2004.

French, N. H. F., Kasischke, E. S., and Williams, D. G.: Variability in the emission of carbon-based trace gases from wildfire in the Alaskan boreal forest, *J. Geophys. Res.*, 108, 8151, doi:10.1029/2001JD000480, 2003.

French, N. H. F., Kasischke, E. S., Hall, R. J., Murphy, K. A., Verbyla, D. L., Hoy, E. E., and Allen, J. L.: Using Landsat data to assess fire and burn severity in the North American boreal forest region: an overview and summary of results, *Int. J. Wildland Fire*, 17, 443–462, doi:10.1071/WF08007, 2008.

French, N. H. F., de Groot, W. J., Jenkins, L. K., Rogers, B. M., Alvarado, E., Amiro, B., de Jong, B., Goetz, S., Hoy, E., Hyer, E., Keane, R., Law, B. E., McKenzie, D., McNulty, S. G., Ottmar, R., Pérez-Salicrup, D. R., Randerson, J., Robertson, K. M., and Turetsky, M.: Model comparisons for estimating carbon emissions from North American wildland fire, *J. Geophys. Res.*, 116, G00K05, doi:10.1029/2010JG001469, 2011.

Giglio, L., Descloitres, J., Justice, C. O., and Kaufman, Y. J.: An enhanced contextual fire detection algorithm for MODIS, *Remote Sens. Environ.*, 87, 273–282, doi:10.1016/S0034-4257(03)00184-6, 2003.

Giglio, L., Csiszar, I., and Justice, C. O.: Global distribution and seasonality of active fires as observed with the terra and aqua Moderate Resolution Imaging Spectroradiometer (MODIS) sensors, *J. Geophys. Res.*, 111, G02016, doi:10.1029/2005JG000142, 2006.

Giglio, L., Randerson, J. T., and van der Werf, G. R.: Analysis of daily, monthly, and annual burned area using the fourth-generation global fire emissions database (GFED4), *J. Geophys. Res.-Biogeo.*, 118, 317–328, doi:10.1002/jgrg.20042, 2013.

Gillett, N. P., Weaver, A. J., Zwiers, F. W., and Flannigan, M. D.: Detecting the effect of climate change on Canadian forest fires, *Geophys. Res. Lett.*, 31, L18211, doi:10.1029/2004GL020876, 2004.

## Daily burned area and carbon emissions from boreal fires in Alaska

S. Veraverbeke et al.

Title Page

Abstract

Introduction

Conclusions

References

Tables

Figures



Back

Close

Full Screen / Esc

Printer-friendly Version

Interactive Discussion



- Goetz, S. J., Sun, M., Baccini, A., and Beck, P. S. A.: Synergistic use of spaceborne lidar and optical imagery for assessing forest disturbance: an Alaska case study, *J. Geophys. Res.*, 115, G00E07, doi:10.1029/2008JG000898, 2010.
- Hall, R. J., Freeburn, J. T., de Groot, W. J., Pritchard, J. M., Lynham, T. J., and Landry, R.: Remote sensing of burn severity: experience from western Canada boreal fires, *Int. J. Wildland Fire*, 17, 476–489, doi:10.1071/WF08013, 2008.
- Hansen, M. C., DeFries, R. S., Townshend, J. R. G., Carroll, M., Dimiceli, C., and Sohlberg, R. A.: Global Percent Tree Cover at a Spatial Resolution of 500 Meters: first Results of the MODIS Vegetation Continuous Fields Algorithm, *Earth Interact.*, 7, 1–15, 2003.
- Hollingsworth, T. N., Walker, M. D., Chapin III, F. S., and Parsons, A. L.: Scale-dependent environmental controls over species composition in Alaskan black spruce communities, *Can. J. For. Res.*, 36, 1781–1796, doi:10.1139/x06-061, 2006.
- Hoy, E. E., French, N. H. F., Turetsky, M. R., Trigg, S. N., and Kasischke, E. S.: Evaluating the potential of Landsat TM/ETM+ imagery for assessing fire severity in Alaskan black spruce forests, *Int. J. Wildland Fire*, 17, 500–514, doi:10.1071/WF08107, 2008.
- Hu, F. S., Higuera, P. E., Walsh, J. E., Chapman, W. L., Duffy, P. A., Brubaker, L. B., and Chipman, M. L.: Tundra burning in Alaska: linkages to climatic change and sea ice retreat, *J. Geophys. Res.*, 115, G04002, doi:10.1029/2009JG001270, 2010.
- Hudak, A. T., Morgan, P., Bobbitt, M. J., Smith, A. M. S., Lewis, S. A., Lentile, L. B., Robichaud, P. R., Clark, J. T., and McKinley, R. A.: The relationship of multispectral satellite imagery to immediate fire effects, *Fire Ecol.*, 3, 64–90, 2007.
- Huete, A., Didan, K., Miura, T., Rodriguez, E., Gao, X., and Ferreira, L.: Overview of the radiometric and biophysical performance of the MODIS vegetation indices, *Remote Sens. Environ.*, 83, 195–213, doi:10.1016/S0034-4257(02)00096-2, 2002.
- Hyer, E. J., Kasischke, E. S., and Allen, D. J.: Effects of source temporal resolution on transport simulations of boreal fire emissions, *J. Geophys. Res.*, 112, D01302, doi:10.1029/2006JD007234, 2007.
- Jin, Y., Randerson, J. T., Goetz, S. J., Beck, P. S. A., Loranty, M. M., and Goulden, M. L.: The influence of burn severity on postfire vegetation recovery and albedo change during early succession in North American boreal forests, *J. Geophys. Res.*, 117, G01036, doi:10.1029/2011JG001886, 2012.

## Daily burned area and carbon emissions from boreal fires in Alaska

S. Veraverbeke et al.

Title Page

Abstract

Introduction

Conclusions

References

Tables

Figures

⏪

⏩

◀

▶

Back

Close

Full Screen / Esc

Printer-friendly Version

Interactive Discussion



Jin, Y., Randerson, J. T., Faivre, N., Capps, S., Hall, A., and Goulden, M. L.: Contrasting controls on wildland fires in Southern California during periods with and without Santa Ana winds, *J. Geophys. Res.-Biogeo.*, 119, 432–450, doi:10.1002/2013JG002541, 2014.

Johnstone, J. F. and Kasischke, E. S.: Stand-level effects of soil burn severity on postfire regeneration in a recently burned black spruce forest, *Can. J. For. Res.*, 35, 2151–2163, doi:10.1139/x05-087, 2005.

Johnstone, J. F., Hollingsworth, T. N., Chapin, F. S., and Mack, M. C.: Changes in fire regime break the legacy lock on successional trajectories in Alaskan boreal forest, *Glob. Change Biol.*, 16, 1281–1295, doi:10.1111/j.1365-2486.2009.02051.x, 2010.

Jones, B. M., Kolden, C. A., Jandt, R., Abatzoglou, J. T., Urban, F., and Arp, C. D.: Fire behavior, weather, and burn severity of the 2007 Anaktuvuk River Tundra Fire, North Slope, Alaska, *Arctic, Antarct. Alp. Res.*, 41, 309–316, doi:10.1657/1938-4246-41.3.309, 2009.

Kajii, Y., Kato, S., Streets, D. G., Tsai, N. Y., Shvidenko, A., Nilsson, S., McCallum, I., Minko, N. P., Abushenko, N., Altyntsev, D., and Khodzer, T. V.: Boreal forest fires in Siberia in 1998: Estimation of area burned and emissions of pollutants by advanced very high resolution radiometer satellite data, *J. Geophys. Res.*, 107, 4745, doi:10.1029/2001JD001078, 2002.

Kane, E. S., Valentine, D. W., Schuur, E. A., and Dutta, K.: Soil carbon stabilization along climate and stand productivity gradients in black spruce forests of interior Alaska, *Can. J. For. Res.*, 35, 2118–2129, doi:10.1139/x05-093, 2005.

Kane, E. S., Kasischke, E. S., Valentine, D. W., Turetsky, M. R., and McGuire, A. D.: Topographic influences on wildfire consumption of soil organic carbon in interior Alaska: implications for black carbon accumulation, *J. Geophys. Res.*, 112, G03017, doi:10.1029/2007JG000458, 2007.

Kasischke, E. S. and Bruhwiler, L. P.: Emissions of carbon dioxide, carbon monoxide, and methane from boreal forest fires in 1998, *J. Geophys. Res.*, 108, 8146, doi:10.1029/2001JD000461, 2002.

Kasischke, E. S. and Hoy, E. E.: Controls on carbon consumption during Alaskan wildland fires, *Glob. Change Biol.*, 18, 685–699, doi:10.1111/j.1365-2486.2011.02573.x, 2012.

Kasischke, E. S. and Johnstone, J. F.: Variation in postfire organic layer thickness in a black spruce forest complex in interior Alaska and its effects on soil temperature and moisture, *Can. J. For. Res.*, 35, 2164–2177, doi:10.1139/x05-159, 2005.

## Daily burned area and carbon emissions from boreal fires in Alaska

S. Veraverbeke et al.

[Title Page](#)

[Abstract](#)

[Introduction](#)

[Conclusions](#)

[References](#)

[Tables](#)

[Figures](#)

[⏪](#)

[⏩](#)

[◀](#)

[▶](#)

[Back](#)

[Close](#)

[Full Screen / Esc](#)

[Printer-friendly Version](#)

[Interactive Discussion](#)



- Kasischke, E. S. and Turetsky, M. R.: Recent changes in the fire regime across the North American boreal region – Spatial and temporal patterns of burning across Canada and Alaska, *Geophys. Res. Lett.*, 33, L09703, doi:10.1029/2006GL025677, 2006.
- Kasischke, E. S., French, N. H. F., Bourgeau-Chavez, L. L., and Christensen, N. L.: Estimating release of carbon from 1990 and 1991 forest fires in Alaska, *J. Geophys. Res.*, 100, 2941, doi:10.1029/94JD02957, 1995.
- Kasischke, E. S., Williams, D., and Barry, D.: Analysis of the patterns of large fires in the boreal forest region of Alaska, *Int. J. Wildland Fire*, 11, 131–144, doi:10.1071/WF02023, 2002.
- Kasischke, E. S., Turetsky, M. R., Ottmar, R. D., French, N. H. F., Hoy, E. E., and Kane, E. S.: Evaluation of the composite burn index for assessing fire severity in Alaskan black spruce forests, *Int. J. Wildland Fire*, 17, 515–526, doi:10.1071/WF08002, 2008.
- Kasischke, E. S., Loboda, T., Giglio, L., French, N. H. F., Hoy, E. E., de Jong, B., and Riano, D.: Quantifying burned area for North American forests: implications for direct reduction of carbon stocks, *J. Geophys. Res.*, 116, G04003, doi:10.1029/2011JG001707, 2011.
- Kasischke, E. S., Verbyla, D. L., Rupp, T. S., McGuire, A. D., Murphy, K. A., Jandt, R., Barnes, J. L., Hoy, E. E., Duffy, P. A., Calef, M., and Turetsky, M. R.: Alaska's changing fire regime – implications for the vulnerability of its boreal forests, *Can. J. For. Res.*, 40, 1313–1324, doi:10.1139/X10-098, 2010.
- Keeley, J. E.: Fire intensity, fire severity and burn severity: a brief review and suggested usage, *Int. J. Wildland Fire*, 18, 116–126, doi:10.1071/WF07049, 2009.
- Key, C. H. and Benson, N. C.: Landscape assessment: ground measure of severity; the Composite Burn Index, and remote sensing of severity, the Normalized Burn Index, in: FIREMON: Fire Effects Monitoring and Inventory System, edited by: Lutes, D., Keane, R., Caratti, J., Key, C., Benson, N., Sutherland, S., and Grangi, L., USDA Forest Service, Fort Collins, CO, 1–51, 2006.
- Kolden, C. A. and Abatzoglou, J. T.: Wildfire consumption and interannual impacts by land cover in Alaskan boreal forest, *Fire Ecol.*, 7, 98–114, doi:10.4996/fireecology.0801098, 2012.
- Kolden, C. A. and Rogan, J.: Mapping Wildfire Burn Severity in the Arctic Tundra from Downsampled MODIS Data, *Arctic, Antarct. Alp. Res.*, 45, 64–76, doi:10.1657/1938-4246-45.1.64, 2013.
- Kolden, C. A., Lutz, J. A., Key, C. H., Kane, J. T., and van Wagtenonk, J. W.: Mapped vs. actual burned area within wildfire perimeters: characterizing the unburned, *For. Ecol. Manage.*, 286, 38–47, doi:10.1016/j.foreco.2012.08.020, 2012.



## Daily burned area and carbon emissions from boreal fires in Alaska

S. Veraverbeke et al.

Title Page

Abstract

Introduction

Conclusions

References

Tables

Figures

◀

▶

◀

▶

Back

Close

Full Screen / Esc

Printer-friendly Version

Interactive Discussion



- Ottmar, R. D., Sandberg, D. V., Riccardi, C. L., and Prichard, S. J.: An overview of the Fuel Characteristic Classification System – quantifying, classifying, and creating fuelbeds for resource planning, *Can. J. For. Res.*, 37, 2383–2393, doi:10.1139/X07-077, 2007.
- Parks, S. A.: Mapping day-of-burning with coarse-resolution satellite fire-detection data, *Int. J. Wildland Fire*, 23, 215–223, doi:10.1071/WF13138, 2014.
- Pimont, F., Dupuy, J.-L., and Linn, R. R.: Coupled slope and wind effects on fire spread with influences of fire size: a numerical study using FIRETEC, *Int. J. Wildland Fire*, 21, 828–842, doi:10.1071/WF11122, 2012.
- Randerson, J. T., Chen, Y., van der Werf, G. R., Rogers, B. M., and Morton, D. C.: Global burned area and biomass burning emissions from small fires, *J. Geophys. Res.*, 117, G04012, doi:10.1029/2012JG002128, 2012.
- Randerson, J. T., Liu, H., Flanner, M. G., Chambers, S. D., Jin, Y., Hess, P. G., Pfister, G., Mack, M. C., Treseder, K. K., Welp, L. R., Chapin, F. S., Harden, J. W., Goulden, M. L., Lyons, E., Neff, J. C., Schuur, E. A. G., and Zender, C. S.: The impact of boreal forest fire on climate warming, *Science*, 314, 1130–1132, doi:10.1126/science.1132075, 2006.
- Riccardi, C. L., Ottmar, R. D., Sandberg, D. V., Andreu, A., Elman, E., Kopper, K., and Long, J.: The fuelbed: a key element of the fuel characteristic classification system, *Can. J. For. Res.*, 37, 2394–2412, doi:10.1139/X07-143, 2007.
- Rocha, A. V., Loranty, M. M., Higuera, P. E., Mack, M. C., Hu, F. S., Jones, B. M., Breen, A. L., Rastetter, E. B., Goetz, S. J., and Shaver, G. R.: The footprint of Alaskan tundra fires during the past half-century: implications for surface properties and radiative forcing, *Environ. Res. Lett.*, 7, 044039, doi:10.1088/1748-9326/7/4/044039, 2012.
- Rogers, B. M., Randerson, J. T., and Bonan, G. B.: High-latitude cooling associated with landscape changes from North American boreal forest fires, *Biogeosciences*, 10, 699–718, doi:10.5194/bg-10-699-2013, 2013.
- Rogers, B. M., Veraverbeke, S., Azzari, G., Czimczik, C. I., Holden, S. R., Mouteva, G. O., Sedano, F., Treseder, K. K., and Randerson, J. T.: Quantifying fire-wide carbon emissions in interior Alaska using field measurements and Landsat imagery, *J. Geophys. Res.*, 119, 1608–1629, 2014.
- Rothermel, R. C.: A mathematical model for predicting fire spread in wildland fuels, Ogden, UT, Project No. INT-115, 1972.
- Roy, D. P., Ju, J., Kline, K., Scaramuzza, P. L., Kovalsky, V., Hansen, M., Loveland, T. R., Vermote, E., and Zhang, C.: Web-enabled Landsat Data (WELD): Landsat ETM+

## Daily burned area and carbon emissions from boreal fires in Alaska

S. Veraverbeke et al.

[Title Page](#)

[Abstract](#)

[Introduction](#)

[Conclusions](#)

[References](#)

[Tables](#)

[Figures](#)

[⏪](#)

[⏩](#)

[◀](#)

[▶](#)

[Back](#)

[Close](#)

[Full Screen / Esc](#)

[Printer-friendly Version](#)

[Interactive Discussion](#)



composited mosaics of the conterminous United States, *Remote Sens. Environ.*, 114, 35–49, doi:10.1016/j.rse.2009.08.011, 2010.

Sedano, F. and Randerson, J. T.: Multi-scale influence of vapor pressure deficit on fire ignition and spread in boreal forest ecosystems, *Biogeosciences*, 11, 3739–3755, doi:10.5194/bg-11-3739-2014, 2014.

Seiler, W. and Crutzen, P. J.: Estimates of gross and net fluxes of carbon between the biosphere and the atmosphere from biomass burning, *Climatic Change*, 2, 207–247, doi:10.1007/BF00137988, 1980.

Sexton, J. O., Song, X.-P., Feng, M., Noojipady, P., Anand, A., Huang, C., Kim, D.-H., Collins, K. M., Channan, S., DiMiceli, C., and Townshend, J. R.: Global, 30 m resolution continuous fields of tree cover: landsat-based rescaling of MODIS vegetation continuous fields with lidar-based estimates of error, *International Journal of Digital Earth*, 6, 427–448, doi:10.1080/17538947.2013.786146, 2013.

Soja, A. J., Cofer, W. R., Shugart, H. H., Sukhinin, A. I., Stackhouse Jr., P. W., McRae, D. J., and Conard, S. J.: Estimating fire emissions and disparities in boreal Siberia (1998–2002), *J. Geophys. Res.*, 109, D14S06, doi:10.1029/2004JD004570, 2004.

Soverel, N. O., Perrakis, D. D. B., and Coops, N. C.: Estimating burn severity from Landsat dNBR and RdNBR indices across western Canada, *Remote Sens. Environ.*, 114, 1896–1909, doi:10.1016/j.rse.2010.03.013, 2010.

Tachikawa, T., Kabu, M., Iwasaki, A., Gesch, D., Oimoen, M., Zhang, Z., Danielson, J., Krieger, T., Curtis, B., Haase, J., Abrams, M., Crippen, R., and Carabajal, C.: ASTER Global Digital Elevation Model Version 2 – Summary of Validation Results, 2011.

Tan, Z., Tieszen, L. T., Zhu, Z., Liu, S., and Howard, S. M.: An estimate of carbon emissions from 2004 wildfires across Alaskan Yukon River Basin, *Carbon Balance and Management*, 2, 1–8, 2007.

Tosca, M. G., Randerson, J. T., and Zender, C. S.: Global impact of smoke aerosols from landscape fires on climate and the Hadley circulation, *Atmos. Chem. Phys.*, 13, 5227–5241, doi:10.5194/acp-13-5227-2013, 2013.

Turetsky, M. R., Kane, E. S., Harden, J. W., Ottmar, R. D., Manies, K. L., Hoy, E., and Kasischke, E. S.: Recent acceleration of biomass burning and carbon losses in Alaskan forests and peatlands, *Nat. Geosci.*, 4, 27–31, doi:10.1038/ngeo1027, 2011.

van der Werf, G. R., Randerson, J. T., Giglio, L., Collatz, G. J., Mu, M., Kasibhatla, P. S., Morton, D. C., DeFries, R. S., Jin, Y., and van Leeuwen, T. T.: Global fire emissions and

## Daily burned area and carbon emissions from boreal fires in Alaska

S. Veraverbeke et al.

Title Page

Abstract

Introduction

Conclusions

References

Tables

Figures



Back

Close

Full Screen / Esc

Printer-friendly Version

Interactive Discussion

the contribution of deforestation, savanna, forest, agricultural, and peat fires (1997–2009), *Atmos. Chem. Phys.*, 10, 11707–11735, doi:10.5194/acp-10-11707-2010, 2010.

Van Wagner, C. E.: Development and structure of the Canadian forest Fire Weather Index system, Canadian Forestry Service, Ottawa, 1987.

5 Van Wagtendonk, J. W., Root, R. R., and Key, C. H.: Comparison of AVIRIS and Landsat ETM+ detection capabilities for burn severity, *Remote Sens. Environ.*, 92, 397–408, doi:10.1016/j.rse.2003.12.015, 2004.

Veraverbeke, S. and Hook, S. J.: Evaluating spectral indices and spectral mixture analysis for assessing fire severity, combustion completeness and carbon emissions, *Int. J. Wildland Fire*, 22, 707–720, doi:10.1071/WF12168, 2013.

10 Veraverbeke, S., Lhermitte, S., Verstraeten, W. W., and Goossens, R.: The temporal dimension of differenced Normalized Burn Ratio (dNBR) fire/burn severity studies: the case of the large 2007 Peloponnese wildfires in Greece, *Remote Sens. Environ.*, 114, 2548–2563, doi:10.1016/j.rse.2010.05.029, 2010.

15 Veraverbeke, S., Sedano, F., Hook, S. J., Randerson, J. T., Jin, Y., and Rogers, B. M.: Mapping the daily progression of large wildland fires using MODIS active fire data, *Int. J. Wildland Fire*, 23, 655–667, 2014.

Verbyla, D. and Lord, R.: Estimating post-fire organic soil depth in the Alaskan boreal forest using the Normalized Burn Ratio, *Int. J. Remote Sens.*, 29, 3845–3853, doi:10.1080/01431160701802497, 2008.

Viereck, L. A.: Wildfire in the Taiga of Alaska, *Quaternary Research*, 3, 465–495, 1973.

20 Yokelson, R. J., Burling, I. R., Gilman, J. B., Warneke, C., Stockwell, C. E., de Gouw, J., Akagi, S. K., Urbanski, S. P., Veres, P., Roberts, J. M., Kuster, W. C., Reardon, J., Griffith, D. W. T., Johnson, T. J., Hosseini, S., Miller, J. W., Cocker III, D. R., Jung, H., and Weise, D. R.: Coupling field and laboratory measurements to estimate the emission factors of identified and unidentified trace gases for prescribed fires, *Atmos. Chem. Phys.*, 13, 89–116, doi:10.5194/acp-13-89-2013, 2013.

## Daily burned area and carbon emissions from boreal fires in Alaska

S. Veraverbeke et al.

[Title Page](#)

[Abstract](#)

[Introduction](#)

[Conclusions](#)

[References](#)

[Tables](#)

[Figures](#)



[Back](#)

[Close](#)

[Full Screen / Esc](#)

[Printer-friendly Version](#)

[Interactive Discussion](#)



**Table 1.** Environmental variables selected to predict ground layer consumption by fire in black spruce forest. The pre-fire tree cover and dNBR layers were also used to predict the aboveground consumption.

Variable	Rationale	Data
elevation (m)	Elevation regulates soil organic layer thickness, carbon density, drainage conditions and seasonal timing of permafrost thaw (Kane et al., 2005, 2007; Kasischke and Johnstone, 2005; Barrett et al., 2010; Kasischke and Hoy, 2012)	ASTER GDEM 2 (Tachikawa et al., 2011).
slope (°)	Slope regulates drainage conditions, organic layer thickness and fire behavior. Sloped terrain is generally better drained than flat terrain (Barrett et al., 2011). Steepness of the terrain regulates tree establishment (Hollingsworth et al., 2006) and fire spread rates and severity (Rothermel, 1972).	derived from ASTER GDEM 2
northness – cosine of aspect	Northness regulates drainage conditions, organic layer thickness and carbon density. Wetness increases with northness, solar insolation decreases with northness. North-oriented slopes are wetter and colder than south-faced slopes and have thicker, (Kane et al., 2007; Turetsky et al., 2011).	derived from ASTER GDEM 2
pre-fire tree cover (%)	Pre-fire tree cover determines the available biomass for aboveground consumption. Aboveground consumption relates to belowground consumption (Rogers et al., 2014). Pre-fire tree cover is also a proxy of stand age, and thus of the thickness, density and wetness of the soil organic layer (Kasischke and Johnstone, 2005; Beck et al., 2011b; Rogers et al., 2013).	tree cover continuous fields 30 m: Sexton et al. (2013) 250 m: Hansen et al. (2003)
time of burning (day of the year)	Time of burning influences the dryness of the soil organic layer during the season (Turetsky et al., 2011; Kasischke and Hoy, 2012)	derived from MODIS active fire data
dNBR	dNBR assesses pre-/post-fire changes in near shortwave infrared reflectance, which relate to changes in vegetation abundance, charcoal deposition and soil exposure (López García and Caselles, 1991; van Wagtenonk et al., 2004; Key and Benson, 2006)	30 m: MTBS (Eidenshink et al., 2007) 500 m: derived from MODIS surface reflectance

ASTER GDEM 2: Advanced Spaceborne Thermal Emission and Reflection Radiometer Global Digital Elevation Model Version 2 (downloaded from <http://reverb.echo.nasa.gov>, last access: 25 November 2014).

dNBR: differenced Normalized Burn Ratio.

MODIS: Moderate Resolution Imaging Spectroradiometer.

MTBS: Monitoring Trends in Burn Severity (downloaded from <http://www.mtbs.gov/>, last access: 25 November 2014).

Tree cover data downloaded from <http://glcf.umd.edu/data/landsatTreecover/> (30 m), and <http://reverb.echo.nasa.gov> (500 m), MODIS surface reflectance data from <http://reverb.echo.nasa.gov>, MODIS active fire data from <ftp://fuoco.geog.umd.edu/modis> (all last access: on 25 November 2014).

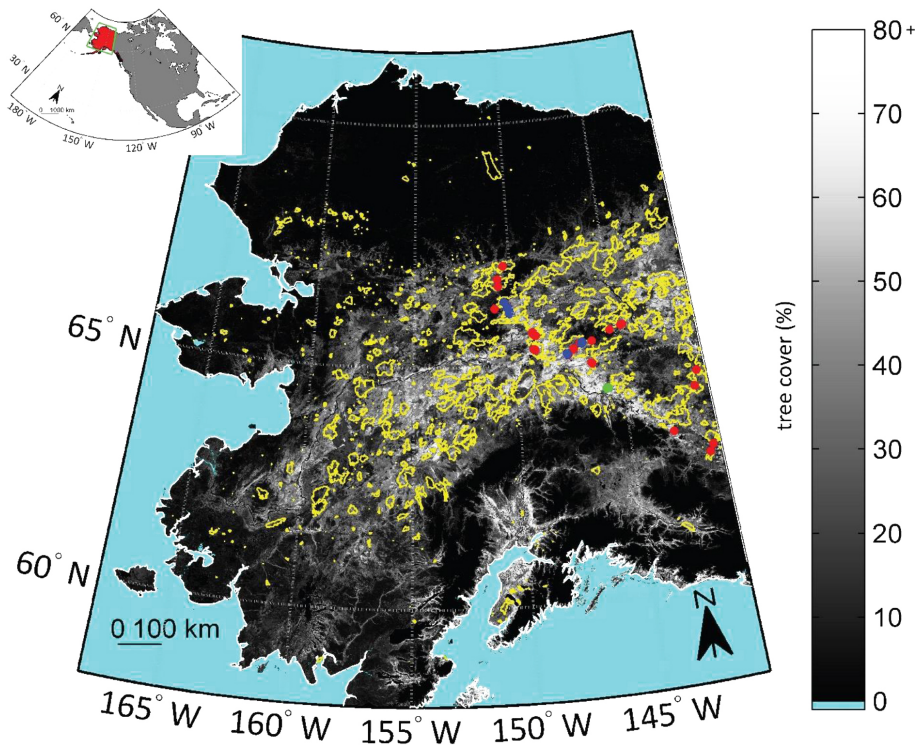


**Figure 1.** Fires that occurred in the study area between 2001 and 2012 (yellow perimeters) from the Alaska Large Fire Database. The background tree cover map is the Moderate Resolution Imaging Spectroradiometer Vegetation Continuous Fields product (MOD44B, Hansen et al., 2003) for the year 2000. The colored dots represent the location of field plots from Turetsky et al. (2011) (red), Boby et al. (2010) (blue) and Rogers et al. (2014) (green). Note that at the scale of the map, some field plot locations overlap due to their close proximity to each other.

**Daily burned area and carbon emissions from boreal fires in Alaska**

S. Veraverbeke et al.

<a href="#">Title Page</a>	
<a href="#">Abstract</a>	<a href="#">Introduction</a>
<a href="#">Conclusions</a>	<a href="#">References</a>
<a href="#">Tables</a>	<a href="#">Figures</a>
<a href="#">◀</a>	<a href="#">▶</a>
<a href="#">◀</a>	<a href="#">▶</a>
<a href="#">Back</a>	<a href="#">Close</a>
<a href="#">Full Screen / Esc</a>	
<a href="#">Printer-friendly Version</a>	
<a href="#">Interactive Discussion</a>	



## Daily burned area and carbon emissions from boreal fires in Alaska

S. Veraverbeke et al.

Title Page

Abstract

Introduction

Conclusions

References

Tables

Figures



Back

Close

Full Screen / Esc

Printer-friendly Version

Interactive Discussion

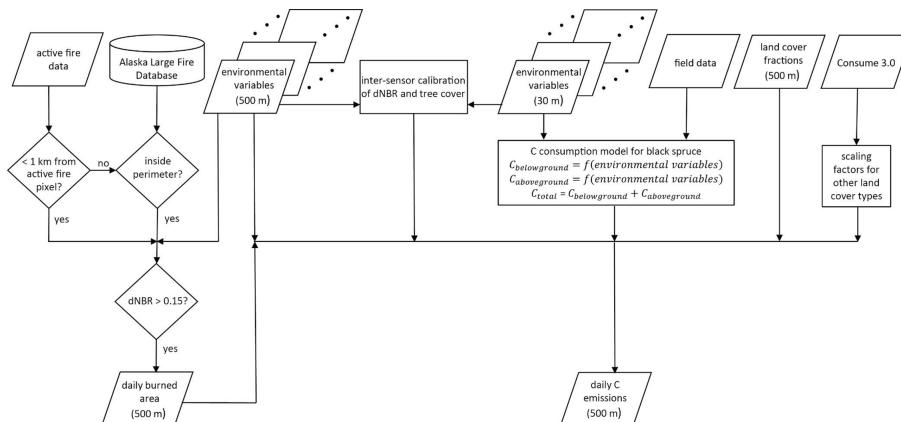


**Figure 2.** Workflow used to obtain daily burned area and carbon emissions in the Alaskan Fire Emissions Database (AKFED) (dNBR: differenced normalized burn ratio).

## Daily burned area and carbon emissions from boreal fires in Alaska

S. Veraverbeke et al.

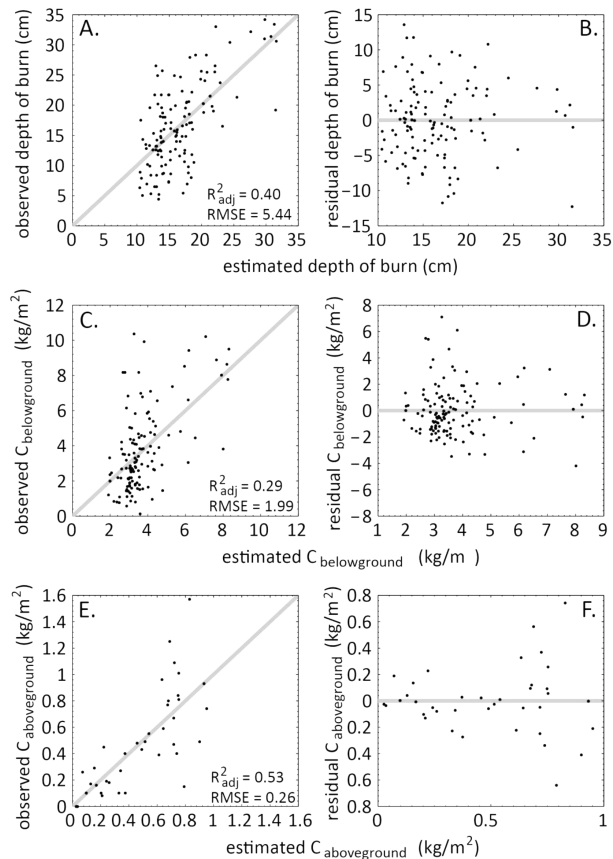


**Figure 3.** Scatter plots between the observed and estimated (a) depth of burn, (c) belowground and (e) aboveground carbon consumption from the multiplicative nonlinear model, and corresponding regression residuals (b, d and f). The grey line represents the 1 : 1 line in the left panels, and the  $y = 0$  line in the right panels. All models were significant at  $p < 0.001$  (RMSE: root mean square error).

## Daily burned area and carbon emissions from boreal fires in Alaska

S. Veraverbeke et al.

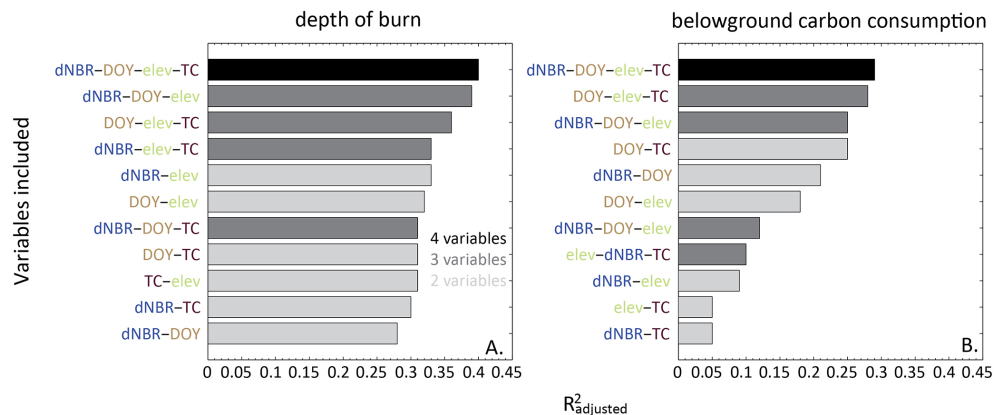


**Figure 4.** Relative importance of variables assessed from the nonlinear multiplicative models using all different combinations of two or more variables for **(a)** depth of burn and **(b)** belowground carbon consumption. (dNBR: differenced normalized burn ratio, DOY: day of the year, tc: tree cover, elev: elevation)

[Title Page](#)
[Abstract](#)
[Introduction](#)
[Conclusions](#)
[References](#)
[Tables](#)
[Figures](#)
[◀](#)
[▶](#)
[◀](#)
[▶](#)
[Back](#)
[Close](#)
[Full Screen / Esc](#)
[Printer-friendly Version](#)
[Interactive Discussion](#)

## Daily burned area and carbon emissions from boreal fires in Alaska

S. Veraverbeke et al.

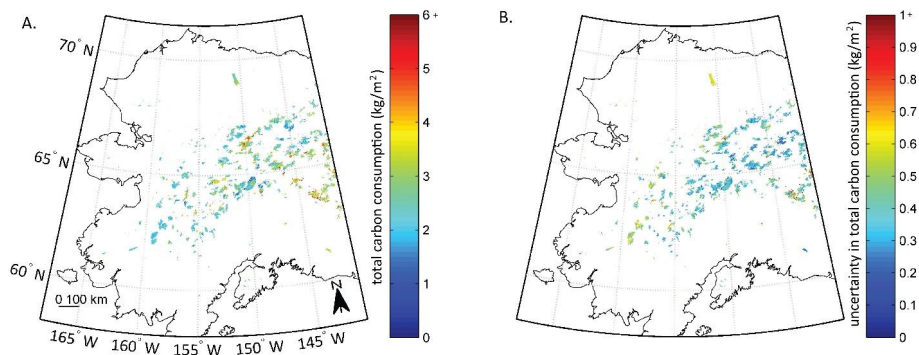


**Figure 5.** (a) Total carbon consumption map by fire and (b) uncertainty, expressed as the SD of the prediction error, for the spatiotemporal domain.

[Title Page](#)[Abstract](#)[Introduction](#)[Conclusions](#)[References](#)[Tables](#)[Figures](#)[◀](#)[▶](#)[◀](#)[▶](#)[Back](#)[Close](#)[Full Screen / Esc](#)[Printer-friendly Version](#)[Interactive Discussion](#)

## Daily burned area and carbon emissions from boreal fires in Alaska

S. Veraverbeke et al.

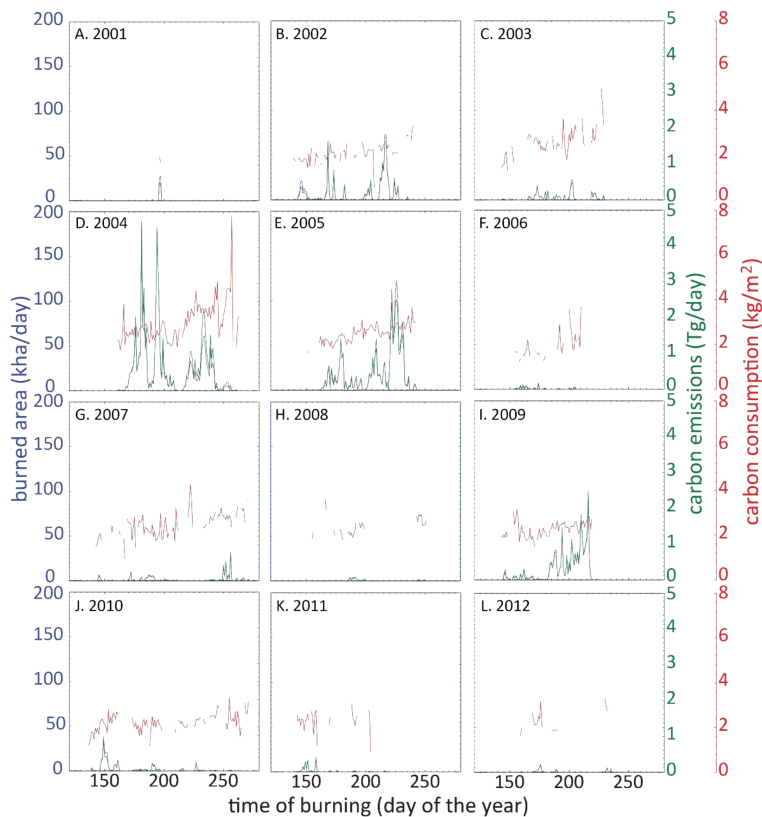


**Figure 6.** Daily burned area, carbon consumption and emissions from Alaska derived from the Alaskan Fire Emissions Database for the years 2001–2012.

[Title Page](#)
[Abstract](#)
[Introduction](#)
[Conclusions](#)
[References](#)
[Tables](#)
[Figures](#)
[◀](#)
[▶](#)
[◀](#)
[▶](#)
[Back](#)
[Close](#)
[Full Screen / Esc](#)
[Printer-friendly Version](#)
[Interactive Discussion](#)


## Daily burned area and carbon emissions from boreal fires in Alaska

S. Veraverbeke et al.

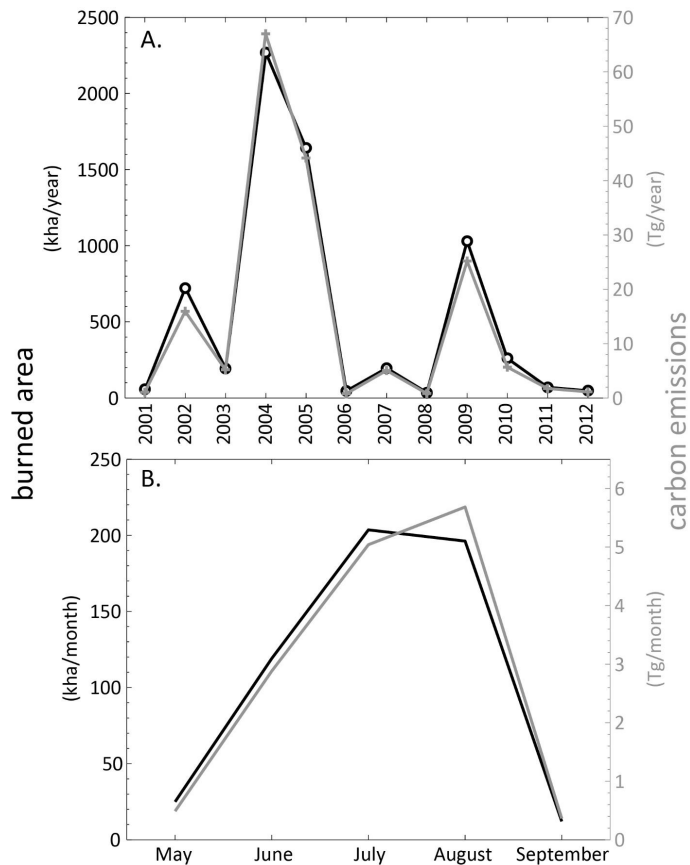


**Figure 7.** (a) Inter- and (b) intra-annual variability in burned area and carbon emissions in Alaska. In (b), the mean monthly burned area and carbon emissions between 2001 and 2012 is plotted.

**Daily burned area and carbon emissions from boreal fires in Alaska**

S. Veraverbeke et al.

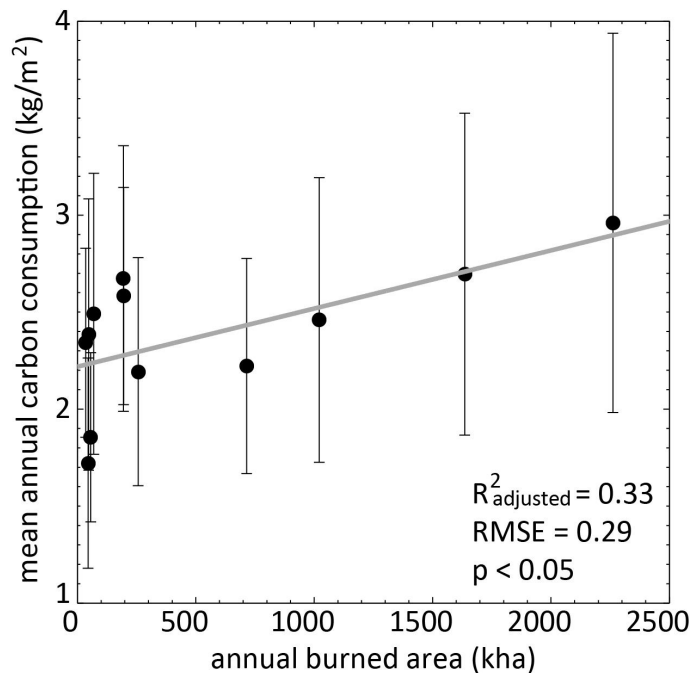


**Figure 8.** Relationship between annual burned area and mean annual carbon consumption. The error bars represent one SD.

[Title Page](#)[Abstract](#)[Introduction](#)[Conclusions](#)[References](#)[Tables](#)[Figures](#)[◀](#)[▶](#)[◀](#)[▶](#)[Back](#)[Close](#)[Full Screen / Esc](#)[Printer-friendly Version](#)[Interactive Discussion](#)

## Daily burned area and carbon emissions from boreal fires in Alaska

S. Veraverbeke et al.

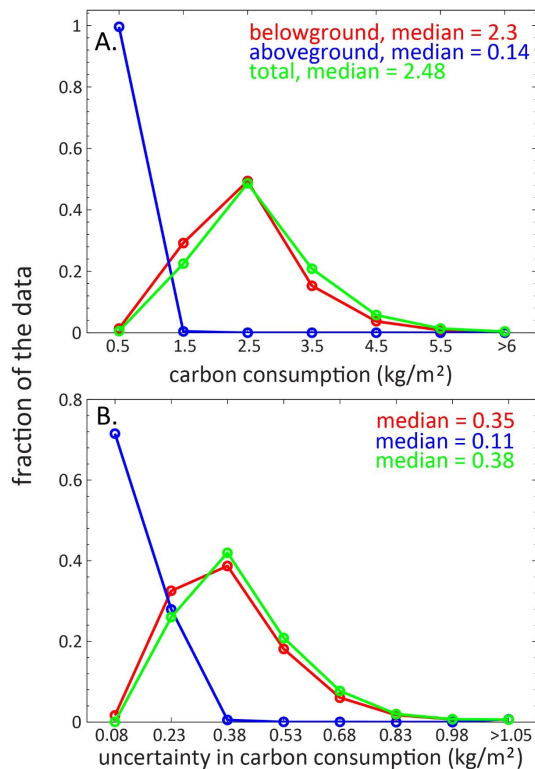


**Figure 9.** Distribution of (a) carbon consumption and (b) pixel-based uncertainties in carbon consumption from the Alaskan Fire Emissions Database between 2001 and 2012. The x axes are labeled with the center of the binning intervals.

Title Page

Abstract

Introduction

Conclusions

References

Tables

Figures

◀

▶

◀

▶

Back

Close

Full Screen / Esc

Printer-friendly Version

Interactive Discussion



## Daily burned area and carbon emissions from boreal fires in Alaska

S. Veraverbeke et al.

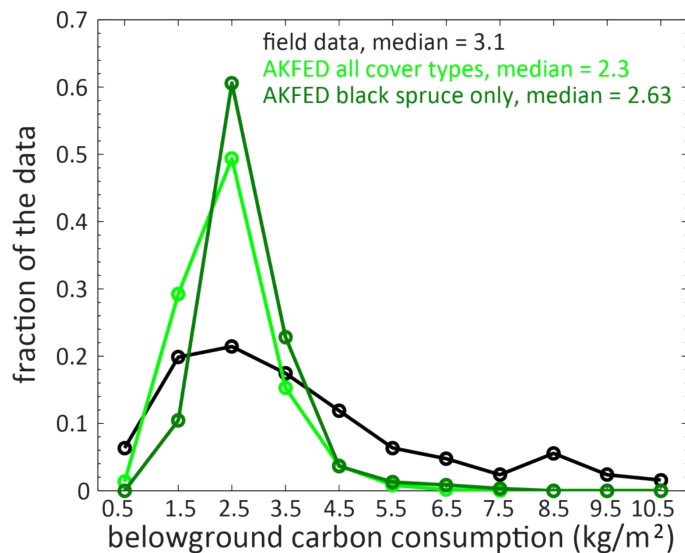


**Figure 10.** Distribution of belowground carbon consumption of field data and the Alaskan Fire Emissions Database (AKFED) between 2001 and 2012. The  $x$  axes are labeled with the center of the binning intervals.

Title Page

Abstract

Introduction

Conclusions

References

Tables

Figures

◀

▶

◀

▶

Back

Close

Full Screen / Esc

Printer-friendly Version

Interactive Discussion

